Silica filled poly(4-methyl-2-pentyne) nanocomposite membranes: Similarities and differences with poly(1-trimethylsilyl-1-propyne)-silica systems

Silica filled poly(4-methyl-2-pentyne) nanocomposite membranes: similarities and differences with poly(1-trimethylsilyl-1-propyne) -silica systems

Kristien De Sitter[1,2], Anna Andersson[3], Jan D'Haen[4,5], Roger Leysen[1], Steven Mullens[1], Frans H. J. Maurer[3], Ivo F. J. Vankelecom[2]

[1] Flemish Institute for Technological Research (VITO), Boeretang 200, B-2400 Mol, Belgium

[2] Centre for Surface Chemistry and Catalysis (COK), Faculty of Bioscience Engineering, Katholieke Universiteit Leuven, Kasteelpark Arenberg 23, B-3001 Leuven, Belgium

[3] Department of Polymer & Materials Chemistry, Lund Institute of Technology, Lund University, P.O. Box 124, SE-221 00 Lund, Sweden

[4] Institute for Materials Research, Hasselt University, Wetenschapspark 1, B-3590 Diepenbeek, Belgium

[5] IMEC vzw, Division IMOMEC, Wetenschapspark 1, B-3590 Diepenbeek, Belgium

Abstract

The performance of poly(4-methyl-2-pentyne) (PMP)/silica nanocomposites was studied for membranes with a filler content between 10 and 40 wt%. An increase in permeability and a constant vapor selectivity were measured with increasing filler content. The constant selectivity was in contrast to earlier published results for silica filled poly(1-trimethylsilyl-1-propyne) (PTSMP) membranes. Therefore, a comparison between both materials was made. Free volume sizes and interstitial mesopore sizes were determined by use of positron annihilation lifetime spectroscopy (PALS) and image analysis was performed on TEM pictures of both materials. Although both materials possessed interstitial mesopores, a difference in membrane structure was noticed, explaining the difference in membrane performance.

Keywords

image analysis; positron annihilation; mesopores; gas separation; free volume

Introduction

Polymer membranes in the gas separation industry have attracted much interest in the past decades, mostly because of their potential energy saving capacity compared with more conventional separation techniques. Polyacetylene-based polymers, and especially poly(1-trimethylsilyl-1-propyne) (PTMSP) membranes have been studied intensively for applications in this field [1-3]. PTMSP has a glassy nature at room temperature (T_g > 200 °C) and is characterized by high permeabilities, which are attributed to the high free volume content of the polymer matrix [4, 5]. PTMSP is more permeable to large condensable vapors than to small permanent gas molecules, making the polymer well suited for vapor separation applications like the removal of higher hydrocarbons from hydrogen streams and the recovery of organic vapors from process streams.

A few years ago, Merkel *et al.* [6] discovered that the incorporation of nanoscale, nonporous fumed silica particles into PTMSP can increase the already high permeability of the membrane. This increase resulted in their opinion from the capacity of the silica particles to disrupt the polymer chain packing and thus increasing the free volume available for molecular transport. Our research team performed positron annihilation lifetime spectroscopy (PALS), membrane performance and TEM studies on silica filled PTMSP nanocomposites. An increase in permeability but a decrease in selectivity was measured [7]. Simultaneously, an increase in the mean size of the larger free volume elements in the PTMSP matrix was observed. Also the existence of interstitial mesopores was noticed in the nanocomposite and the as-received fumed silica as well [8]. The interstitial cavities seemed to be situated between the particles of silica aggregates. The existence of these aggregates was confirmed by TEM images. A clear correlation

between the size of the interstitial mesopores and the permeability of the nanocomposite was observed. The presence of the mesopores in the materials explained also the selectivity decrease with increasing filler content, because the vapor could no longer block the pores for the permanent gas.

Another polyacetylene-based polymer is poly(4-methyl-2-pentyne) (PMP). PMP is less permeable, but more stable in time and especially more solvent-resistant than PTMSP, making it more attractive for use in industrial environments [9]. For this polymer, Merkel *et al.* [10] reported an increase in permeability and simultaneously in vapor selectivity, upon incorporation of nanosized silica particles in the polymer matrix. The aim of our study is to gain insight in the structure and gas permeation properties of nano-filled PMP in comparison to our earlier studies on PTMSP nano-composites comprising the same filler particles [7,8].

1. Experimental

1.1 Materials

Poly(4-methyl-2-pentyne) (PMP) was synthesized by Hasselt University, Belgium. The synthesis method for PMP is provided in detail elsewhere [9]. The fumed silica used as filler, Cabosil TS-530, was purchased from Cabot Corporation, Germany. TS-530 is a hydrophobic silica due to a treatment with hexamethyldisilazane. The reported density is 2.2 g/cm^3, the specific surface area 220 m^2/g. The individual particle diameter calculated from the surface area and density when a spherical shape is assumed, is about 12 nm.

The cyclohexane used as solvent for PMP was delivered by Merck. Pure gases for permeability experiments (nitrogen, hydrogen, and methane) as well as the gas mixture containing 2 vol% butane and 98 vol% methane were purchased from Praxair, Belgium.

1.2 Membrane preparation

Dense films of unfilled PMP were prepared by casting a cyclohexane solution (2 wt%) on a glass plate. The plate was covered with a glass dish to slow the rate of solvent evaporation. The films were dried at ambient conditions for 10 days.

Filled PMP films were solvent casted silica-polymer mixtures. These mixtures were prepared as described elsewhere for PTMSP [7]: First, 10 – 40 wt% silica (based on polymer) were dispersed in cyclohexane at room temperature applying ultrasonic treatment for 30 min followed by magnetic stirring for 3h. Secondly, PMP was dissolved in silica/cyclohexane dispersion by stirring with a magnetic stirrer for 4 days. After this, the solution was cast on a glass plate. The drying procedure of dense PMP films was also used for the PMP-silica nanocomposites. The cast membranes had a thickness of around 65 µm.

1.3 Permeability and selectivity measurements

Pure-gas transport properties of filled and unfilled PMP membranes were determined by exposure to nitrogen, hydrogen and methane at the University of Twente in the Netherlands. The variable pressure method as described by Kapantaidakis and Koops was used [11]. Gas permeabilities were determined at a temperature of 35 °C and were

calculated from the pressure increase as a function of time in a calibrated volume at the permeate side.

Also mixed-gas permeation properties of filled and unfilled PMP membranes were determined. A mixture containing 2 vol% butane and 98 vol% methane was used as feed stream. The feed pressure was kept at 3 bar (unless mentioned otherwise), vacuum was installed at the permeate side. The feed and permeate compositions were analyzed with a Perkin-Elmer gas chromatograph equipped with an Alumina F-1 column. The retentate flow rate was set at 150 ml/min.

All measurements were conducted on two membranes simultaneously. The used membrane samples had no permeation history and were two months old.

1.4 Positron annihilation lifetime spectroscopy

The free volume and interstitial cavity sizes in PTMSP nanocomposite membranes and neat materials were investigated by positron annihilation lifetime spectroscopy (PALS). PALS is a technique which probes the free volume cavities by measuring the lifetime of ortho-Positronium (o-Ps) before annihilation at the free volume sites of the polymer.

The lifetime (τ_3) of o-Ps is a direct measurement of the free volume size, according to the Tao-Eldrup equation [12, 13]:

$$\tau_3 = 0.5 \cdot \left(1 - \frac{R}{R_0} + \frac{1}{2\pi} \sin\frac{2\pi \cdot R}{R_0}\right)^{-1} \quad (1)$$

The Tao-Eldrup equation models the free volume in polymers as spherical cavities with a radius R. An o-Ps in a spherical free volume cavity is described as a particle in a spherical potential well with a radius $R_0 = R + \Delta R$, where ΔR is an electron layer with a thickness of 0.166 nm.

All PALS measurements mentioned in this study were performed at the Department of Polymer & Materials Chemistry at Lund University. A salt of ^{22}Na positron source was used, encapsulated between two sheets of Kapton. The source gave a count rate of 60-80 s^{-1} and each spectrum, which were all recorded at ambient conditions, consisted of about 2.5 million counts. The spectra were recorded using a fast-fast coincidence system with CsF crystals. For each sample, five spectra were recorded. The evaluation method POSITRONFIT was used for extracting positron and positronium lifetimes τ, and intensities I, from the measured spectra. POSITRONFIT fits the measured spectra with a model function consisting of a sum of decaying exponentials convoluted with the resolution function of the lifetime spectrometer plus a constant background. A five-component analysis was used to evaluate the spectra of PMP nanocomposites, while a four-component analysis was used for spectra of unfilled PMP and fumed silica. The variance of fit, which gives information about the goodness of the fit, was for all performed analysis close to unity (below 1.1).

1.5 TEM

The TEM samples were cut with a cryo-ultramicrotome. They were investigated with a Philips CM12 transmission electron microscope. The lines in the TEM images were caused by the diamond knife used during the specimen preparation. The bright field images in the TEM mode allowed only absorption and diffraction contrast.

1.6 Image analysis

For performing image analysis on silica aggregates, the procedure described by Mullens *et al.* [14] was followed:

Step 1: Image acquisition

Transmission electron microscopy (TEM) was used for image acquisition. In Figure 1, a TEM picture of a filled polymer and the corresponding histogram were presented. In the ideal case, a clear separation of the pixels of the polymer matrix and the pixels of the silica aggregates should exist. However, in this case the grey values in the aggregates and grey values representing the polymer overlapped. Moreover, grey values of the background (polymer) were not uniform, caused by the wrinkling of the sample due to sample preparation. There was also a problem of edge effects. Therefore, image enhancement was needed.

Step 2: Image enhancement

Image enhancement was needed to obtain sufficient contrast between the polymer matrix (light area) and the silica particles (dark area). The selection of the region of interest excluded edge effects and incomplete representation of certain features by frame limitations. Image defects were suppressed by improvement of contrast and the use of combinations of erosion and dilation (Figure 2). Adjustment of brightness and contrast was performed to obtain background uniformity (Figure 3). In the final enhancement step, the area of the aggregates were filled (Figure 4).

Step 3: Image thresholding

The next step in the image analysis procedure was threshold segmentation, a technique by which pixels that represent the actual feature of interest are identified in the image by selecting a specific range of grey values within the histogram. All the resulting pixels within this grey value range were considered as black, while the remaining pixels were considered as white. A binary image was the result of this step (Figure 5).

Step 4: Identification of the aggregates

Identification of the different aggregates was the result of the performed steps. Colors were used to highlight separated aggregates (Figure 6).

Step 5: Measurements

Once the features were unambiguously identified by the routine, size measurements were performed. Aggregate size distributions were derived from the calculation of the area of the individual aggregates. The area of each aggregate was determined by counting the number of pixels in each aggregate, multiplied by the area of one pixel. The diameter of a circle with the same area as the aggregate was called the equivalent diameter and could be calculated as:

$$D_{eq} = 2 \cdot \sqrt{\frac{area}{\pi}} \qquad (2)$$

The equivalent diameters of the aggregates were classified in a histogram and analyzed statistically.

2. Results and discussion

2.1 Permeability and selectivity of silica filled PMP membranes

In Table 1, the permeability coefficients and ideal selectivities measured for unfilled PMP membranes are summarized. All data are collected with a feed pressure of 3 bar and a feed temperature of 35 °C. The measured values are lower than values reported earlier [3]. Physical aging can be the reason of this discrepancy. The data reported in this work are for aged membranes, the earlier published data are for freshly casted membranes. The ideal selectivities are low compared to those obtained for conventional glassy polymers. This is a known phenomenon for high free volume polymers [2]. For these polymers, in general solubility selectivity dominates over diffusivity selectivity.

Table 2 presents the mixed gas properties of unfilled PMP membranes for a feed mixture containing 2 vol% n-butane in methane. Just like PTMSP, PMP is more permeable for highly condensable gases like n-butane than for methane. The n-butane/methane selectivity value of 5.12 corresponds well with values mentioned by Lokhandwala *et al.* [15], but is lower than other values mentioned in literature by Merkel *et al.* [10] and Pinnau *et al.* [3]. It is slightly higher than the ideal selectivity calculated for low feed pressure (because the partial pressure of n-butane in mixed-gas measurements is low). It seems that the reversed selectivity is based on the dominance of the solubility selectivity. Condensation of n-butane, causing pore-blocking of methane, is not a significant effect under these conditions of feed pressure and temperature. Selectivity values mentioned in literature are measured at lower temperature (25 °C) and higher feed pressure.

Figure 7 presents the nitrogen, hydrogen and methane permeability as a function of the amount of fillers incorporated in the PMP polymer matrix. All permeability coefficients

increase with increasing filler content. This is in contrast with the predictions of a reduced permeability with filler content calculated with the Maxwell model [16, 17], but in line with the results obtained for filled PTMSP membranes. Figure 8 shows the effect of the filler content on the n-butane/methane mixed gas selectivity of the PMP membranes. This selectivity turns out to be independent of filler content. This proves that the increasing permeability is not caused by large defects created by adding silica particles. The constant selectivity is different from the results measured for filled PTMSP membranes [7] and does not confirm the large selectivity increase mentioned by Merkel *et al.* [10].

The relative mixed and single gas methane permeabilities are presented as a function of filler amount in Figure 9. The higher the filler content, the larger the difference is between the mixed gas and the single gas permeability. The permeation of methane seems less hindered by the presence of n-butane when more filler particles are added to the polymer. Such phenomenon has also been observed in silica filled PTMSP membranes [7]. Propane was blocking hydrogen permeation in unfilled PTMSP. Due to the creation of extra pores by incorporating silica, blocking was prevented. Possibly, this is also the case with butane and methane in silica filled PMP membranes. Therefore, it is important to characterize the free volume and the occurrence of additional cavities in nano-filled PMP composites.

2.2 Free volume and interstitial pores

Table 3 summarizes the lifetimes and intensities of the different positron annihilation processes in neat silica, filled and unfilled PMP calculated with POSITRONFIT. Two o-

Ps lifetimes were obtained for the unfilled PMP (τ_3 and τ_4) and three for filled PMP (τ_3, τ_4 and τ_5), similar to the lifetimes found in PTMSP and its nano-composites [10, 18]. The two longest lifetimes in PTMSP have been previously related to two kinds of free volume cavities, namely large cages (τ_4) interconnected with channel-like holes (τ_3) [10, 18]. In unfilled PMP, these two lifetimes are respectively 6.4 and 2.9 ns, which correspond to hole radii of 0.53 and 0.36 nm respectively. Identical silica particles were incorporated both in PMP and PTMSP. Two o-Ps lifetimes were measured in the hydrophobic silica particles. The shorter lifetime (τ_3) originates from o-Ps annihilation from the particles, the longer lifetime (τ_4) is a consequence of o-Ps annihilation in the interstitial cavities of the filler agglomerates. It is relevant for the gas permeation performance to know whether the interstitial pores are still present after preparation of the silica/PMP nanocomposite membranes from solution. PALS also reveals the possible influence of silica particle incorporation on the polymer free volume elements.

The results of the lifetimes of Table 3 are presented in Figure 10 after converting the data to radii by equation 1. The Figure represents the small and large free volume cavity radii in PMP/silica nanocomposites as a function of filler content. There is a minor decrease in radius for the small pores whereas the large pores are unaffected by filler content. The hole radius of the large pores is varying between 0.52 nm and 0.54 nm, but there is no systematic increase measured with increasing filler content. Thus the incorporation of filler particles induces no significant changes in the polymer free volume sizes. In contradiction with our results, an increase of τ_4 of PMP was previously reported by Merkel *et al.* [10] and was ascribed it to a disruption of the polymer chain packing by the filler particles. An increase of the long lifetimes was measured for PTMSP by both

Merkel *et al.* and Winberg *et al.* [6, 8]. For PTMSP, it is noticed that although the polymer free volume size increase was relevant for the permeability of the membrane, the effect of the existence of interstitial mesopores is even more dominant. The existence of the interstitial pores and their increase as function of filler content can explain the increase in permeability measured for silica filled PMP membranes.

From the data summarized in Table 3, the conclusion can be made that there exist additional pores in PMP/silica nanocomposites. The evolution of the radius of these cavities as a function of filler content is presented in Figure 11. The mesopores are still present when the silica particles are incorporated in PMP. These results are similar to the results obtained earlier for silica filled PTMSP membranes [8], also shown in Figure 12. The linear increase is less clear for PMP than for PTMSP. This is caused by the low intensities of the fifth lifetime which lead to larger errors, especially in the PMP membranes with the lowest filler contents. In general, the values measured for PTMSP and PMP are comparable. The mean radius of the mesopores in PTMSP and PMP nano-composites increase in both systems from 1.0 nm to 1.27 nm of fumed silica and is clearly governed by the fraction of particles in the polymer matrix. The data strongly suggest that the interstitial cavities were partially filled with polymer material, caused by the removal of the solvent and collapse of the fumed silica aggregates in the presence of the polymer matrix during preparation of the membranes. The partial filling of the aggregates is more efficient at lower silica content since a larger amount of macromolecules is available per unit filler surface.

2.3 Effect of interstitial cavities on the membrane performance

Earlier reported results for PTMSP-silica membranes showed a clear correlation between the size of the interstitial cavities and the pure gas permeabilities of the membrane [7]. In Figure 12, the nitrogen, hydrogen and methane permeabilities are plotted against the size of the interstitial mesopores, for PMP membranes. The correlation is not as clear as for filled PTMSP membranes. This is probably caused by the larger error measured on the size of the interstitial mesopores for PMP.

As presented in Figure 8, the butane/methane selectivity of the membranes is independent of the amount of filler incorporated in the PMP matrix. Nevertheless, the interstitial mesopores are of such size that no selectivity between butane and methane would be expected. In that case, a decrease of the total membrane selectivity could be anticipated. The intensity is increasing with increasing filler content. It is thus likely that the intensity can be correlated with the amount of aggregates and thus the total amount of interstitial cavities.

2.4 Differences and similarities between PTMSP-silica and PMP-silica membranes

Although PTMSP and PMP are similar polymers, the effect of incorporating hydrophobic silica particles on gas permeation properties is different. The gas permeabilities are increasing with increasing filler content for both systems. For PTMSP, this increase is caused by the increase in free volume and the existence of large interstitial mesopores. For PMP, only the interstitial mesopores are responsible. Also for gas selectivities, a difference is observed between PTMSP and PMP membranes. The propane/hydrogen

selectivity of PTMSP membranes is decreasing when silica particles are added, while the butane/methane selectivity of PMP membranes is not affected. These results suggest that the aggregate structure of the filler particles in the polymer matrix may play a significant role in the differences of performance of the membranes.

2.4.1 TEM and image analysis

In Figure 13, TEM pictures of PMP membranes with 10 and 30 wt% silica are shown. The silica particles are clearly aggregated in the polymer matrix. The size and the amount of aggregates in the membranes are increasing with increasing filler content similar as we have reported earlier for PTMSP silica membranes [7]. At 10 wt% silica content a broad distribution of aggregate sizes can be observed, it can not be ruled out that single dispersed particles also are present.

To investigate the similarities and differences between the two systems quantitatively, image analysis is performed on representative TEM pictures of PTMSP and PMP membranes containing 10 wt% silica. For both samples, 10 % of the total surface of the image is occupied by silica aggregates. In Figure 14, the percentage of the total amount of aggregates with a certain diameter size is presented. In PTMSP, more than 30 % of the aggregates have a diameter above 300 nm. These large aggregates correspond to more than 75 % of the total aggregate surface (Figure 15) and thus aggregate volume. For PMP, only 6 % of the aggregates are of a size larger than 300 nm. The aggregates with a diameter less than 150 nm represent 70 % of the total amount of silica aggregates. This proves that silica aggregates are much smaller in PMP than in PTMSP. This gives a strong indication for the presence of a lower number of interstitial mesopores in filled

PMP in comparison to filled PTMSP. The smaller aggregate size can be correlated with the lower intensities of large interstitial holes measured by positron annihilation lifetime spectroscopy.

2.4.2 Discussion

From TEM and PALS measurements it can be concluded that PTMSP nanocomposites contain more large aggregates and more interstitial cavities than PMP nanocomposites. Gas permeabilities of both materials are increasing with increasing filler content. The increase in permeability dependent on the gas, but the overall order $P(H_2) > P(CH_4) > P(N_2)$ remains. The transport through the membranes is dominated by the permeation through the polymer phase, but the permeability is increased due to additional fast transport through interstitial voids and the change in polymer matrix properties.

For PTMSP, the propane/hydrogen selectivity decreases as a function of filler content due to the presence of the large interstitial holes. This suggests that there is a pathway through the membrane where pore blocking is not efficient. The interstitial mesopores are probably interconnected, forming perculating channels through the thickness of the membrane.

For PMP, no decrease in butane/methane selectivity is observed. From TEM pictures and PALS measurements we have shown that PMP/silica nanocomposites contain fewer large aggregates and less interstitial holes. Consequently, the formation of transport channels through the membrane is unlikely, resulting in a constant selectivity (Figure 8). In Figure 16 a simplified structural model is presented which constitutes two extremes: the formation of perculating aggregate structures on one hand and on the other hand the

formation of homogeneously dispersed aggregate structures. These schematic drawings represent in their extremes parallel (a) and series (b) models for illustrating structure-property relations for composites.

Reason of different nature of aggregates is not totally clear at this moment. The aggregate structure is certainly influenced by the use of different solvents, the surface polarity of the filler particles and the polymers used in the PMP and PTMSP systems. Further research will focus more on this.

3. Conclusions

PMP membranes with different amounts of hydrophobic silica particles were studied. The influence of adding silica particles to the polymer matrix on membrane performance was measured. The addition of hydrophobic silica leads to an increase in permeability. In contrast with the selectivity results published earlier for filled PTMSP membranes [7], mixed gas measurements on PMP show an almost constant vapor selectivity. The polymer free volume is not changing by the incorporation of silica, but interstitial cavities are formed. For PTMSP-silica membranes [8], these cavities are situated between the particles in the silica aggregates. A correlation between the size of the interstitial cavities and the pure gas permeabilities is observed.

TEM studies and image analysis were performed to find an explanation for the difference in selectivity data between PTMSP-silica and PMP-silica. These measurements showed that the difference is caused by different membrane structures of the two materials. Silica particles are much better dispersed in PMP, while PTMSP nanocomposites contain larger aggregates and more interstitial cavities. In PTMSP, the interstitial mesopores are

probably interconnected, forming channels throughout the entire thickness of the membrane. In PMP/silica nanocomposites a constant selectivity is observed indicating the absence of interconnected channels through the thickness of the membranes.

Creating interstitial mesopores in polymer nanocomposites is therefore important to prepare highly permeable membranes, while the aggregate structure has to be carefully designed to avoid selectivity loss. This knowledge can be used to prepare more efficient nanocomposite membranes for the use in gas separation applications.

Acknowledgements

The authors would like to thank the Membrane Technology Group of the University of Twente in the Netherlands for their help with the permeability and selectivity measurements and especially Tymen Visser for the fruitful discussions.

Kristien De Sitter acknowledges VITO for a grant as doctoral research fellow and NanoMemPro for making it possible to visit the University of Twente. Wim Bouwen, Louis Willems and Jos Cooymans are acknowledged for their help with the experimental setup at VITO.

Anna Andersson and Frans H. J. Maurer acknowledge the Swedish Research Council and Perstorp Specialty Chemicals AB for their financial contributions.

The research was partly performed in the framework of an I.A.P.-P.A.I. grant (IAP 6/27) on Supramolecular Catalysis sponsored by the Belgian Federal Government and the project W000105N (Wetenschappelijke onderzoeksgemeenschap: “Structurele en chemische karakterisatie van materialen op micro- en nanoschaal”).

References

[1] I. Pinnau, C. G. Casillas, A. Morisato and B. D. Freeman, Hydrocarbon/Hydrogen Mixed Gas Permeation in Poly(1-trimethylsilyl-1-propyne) (PTMSP), Poly(1-phenyl-1-propyne) (PPP), and PTMSP/PPP Blends, J. Polym. Sci., Part B: Polym. Phys. 34 (1996) 2613.
[2] K. Nagai, T. Masuda, T. Nakagawa, B. D. Freeman and I. Pinnau, Poly[1-(trimethylsilyl)-1-propyne] and related polymers: synthesis, properties and functions, Prog. Polym. Sci. 26 (2001) 721.
[3] I. Pinnau, Z. He and A. Morisato, Synthesis and gas permeation properties of poly(dialkylacetylenes) containing isopropyl-terminated side-chains, J. Membr. Sci. 241 (2004) 363.
[4] I. Pinnau and L. G. Toy, Transport of organic vapors through poly(1-trimethylsilyl-1-propyne), J. Membr. Sci. 116 (1996) 199.
[5] R. Srinivasan, S. R. Auvil and P. M. Burban, Elucidating the mechanism(s) of gas transport in poly[1-(trimethylsilyl)-1-propyne] (PTMSP) membranes, J. Membr. Sci. 86 (1994) 67.
[6] T. C. Merkel, Z. He, I. Pinnau, B. D. Freeman, P. Meakin and A. J. Hill, Effect of Nanoparticles on Gas Sorption and Transport in Poly(1-trimethylsilyl-1-propyne), Macromolecules 36 (2003) 6844.
[7] K. De Sitter, P. Winberg, J. D'Haen, C. Dotremont, R. Leysen, J. A. Martens, S. Mullens, F. H. J. Maurer and I. F. J. Vankelecom, Silica filled poly(1-trimethylsilyl-1-propyne) nanocomposite membranes: Relation between the transport of gases and structural characteristics, Journal of Membrane Science 278 (2006) 83.
[8] P. Winberg, K. Desitter, C. Dotremont, S. Mullens, I. F. J. Vankelecom and F. H. J. Maurer, Free volume and interstitial mesopores in silica filled poly(1-trimethylsilyl-1-propyne) nanocomposites, Macromolecules 38 (2005) 3776.
[9] A. Morisato and I. Pinnau, Synthesis and gas permeation properties of poly(4-methyl-2-pentyne), J. Membr. Sci. 121 (1996) 243.
[10] T. C. Merkel, B. D. Freeman, R. J. Spontak, Z. He, I. Pinnau, P. Meakin and A. J. Hill, Sorption, Transport, and Structural Evidence for Enhanced Free Volume in Poly(4-methyl-2-pentyne)/fumed Silica Nanocomposite Membranes, Chem. Mater. 15 (2003) 109.
[11] G. C. Kapantaidakis and G. H. Koops, High flux polyethersulfone-polyimide blend hollow fiber membranes for gas separation, J. Membr. Sc. 204 (2002) 153.
[12] M. Eldrup, D. Lightbody and J. N. Sherwood, The temperature-dependence of positron lifetimes in solid pivalic acid, Chem. Phys. 63 (1981) 51.
[13] S. J. Tao, Positronium annihilation in molecular substances, J. Chem. Phys. 56 (1972) 5499.
[14] S. Mullens, J. Luyten and J. Zeschky, Characterization of structure and morphology, in M., S.and P., C., (Eds.), Cellular Ceramics, Wiley-VCH Verlag GmbH & co KGaA, Weinheim, 2005, pp. 227-263.
[15] K. Lokhandwala, M. Ringer, T. T. Su, Z. He, I. Pinnau, H. Wijmans, A. Morisato, K. D. Amo, A. R. Da Costa, R. W. Baker, R. Olsen, H. Hassani and T. Rathkamp, Nitrogen removal from natural gas using membranes, Technical Report (1999).

[16] C. Maxwell, Treatise on Electricity and Magnetism, Oxford University Press, London, 1873.
[17] R. M. Barrer, Diffusion and permeation in heterogeneous media, in Crank, J.and Park, G. S., (Eds.), Diffusion in Polymers, Academic Press, New York, 1968.
[18] Y. P. Yampolskii, V. P. Shantarovich, F. P. Chernyakovskii, A. I. Kornilov and N. A. Plate, Estimation of free volume in poly(trimethylsilyl propyne) by positron annihilation and electrochromism methods, J. Appl. Polym. Sci. 47 (1993) 85.

Tables

Table 1: Permeability coefficients and ideal selectivities of unfilled PMP, measured at 35 °C and a pressure difference of 3 bar

Gas	*Permeability (barrer)*	*Ideal selectivity (P_{gas}/P_{N2})*
N_2	600	1
H_2	2700	4.7
CH_4	1200	2.1

Table 2: Mixed gas measurements of unfilled PMP, performed at 35 °C, 3 bar pressure difference and a feed mixture of 2 vol% butane in methane

α (C_4H_{10}/CH_4)	5.1
$P_{mixed}(C_4H_{10})$ (barrer)	2900
$P_{mixed}(CH_4)$ (barrer)	600

Table 3: Lifetimes and intensities of positron annihilation in PMP/silica nanocomposites

filler content (wt%)	τ_1(ns)	τ_2(ns)	τ_3(ns)	τ_4(ns)	τ_5(ns)
TS-530	0.3±0.01	0.8±0.01	3.2±0.1		53±1
0	0.17±0.01	0.43±0.01	2.9±0.1	6.4±0.1	
10	0.16±0.01	0.43±0.01	2.5±0.2	6.1±0.2	30±5
20	0.21±0.01	0.44±0.01	2.5±0.1	6.1±0.3	36±9
30	0.17±0.01	0.45±0.01	2.5±0.2	6.6±0.2	31±2
40	0.17±0.01	0.44±0.01	2.3±0.1	6.3±0.3	39±1
filler content (wt%)	I_1(%)	I_2(%)	I_3(%)	I_4(%))	I_5(%)
TS-530	76.9±0.5	14.1±0.6	4.2±0.1		4.7±0.1
0	14.9±1.3	56.1±1.2	13.5±0.8	15.5±0.9	
10	12.9±1.2	58.2±1.1	9.8±0.9	18.0±0.9	1.1±0.2
20	17.3±2.5	57.4±2.3	13.0±0.7	10.7±0.8	1.7±0.1
30	14.2±1.3	56.3±1.1	9.9±0.7	16.5±0.7	3.2±0.2
40	13.2±0.1	59.9±1.2	11.0±0.5	10.1±0.6	5.9±0.1

Figures

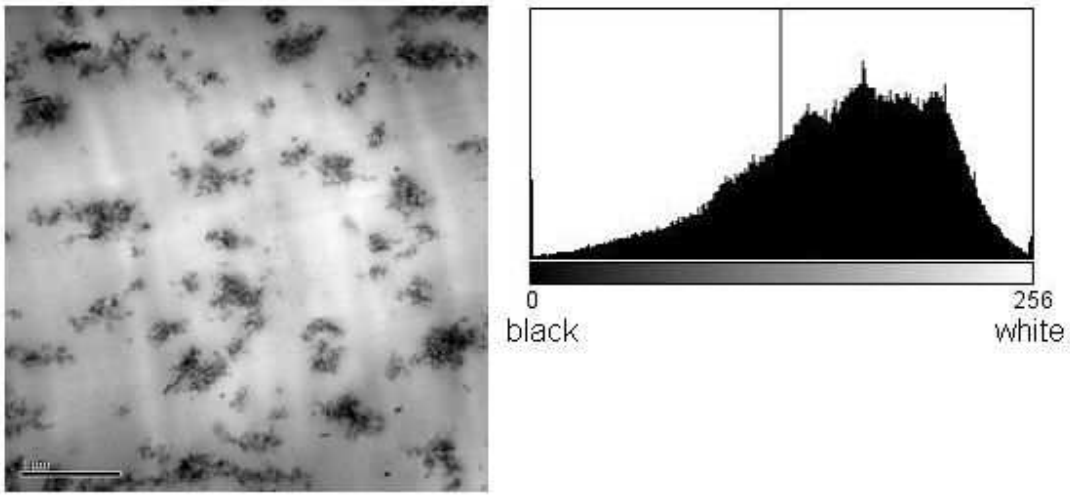

Figure 1: Image analysis step 1 (image acquisition): a TEM picture of a filled polymer and the corresponding histogram

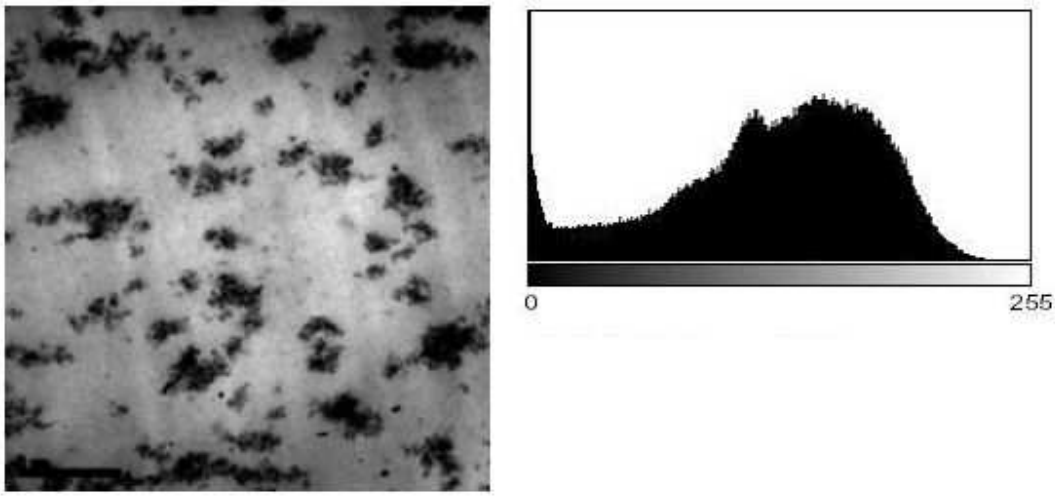

Figure 2: Image analysis step 2a (image enhancement): suppressing image defects

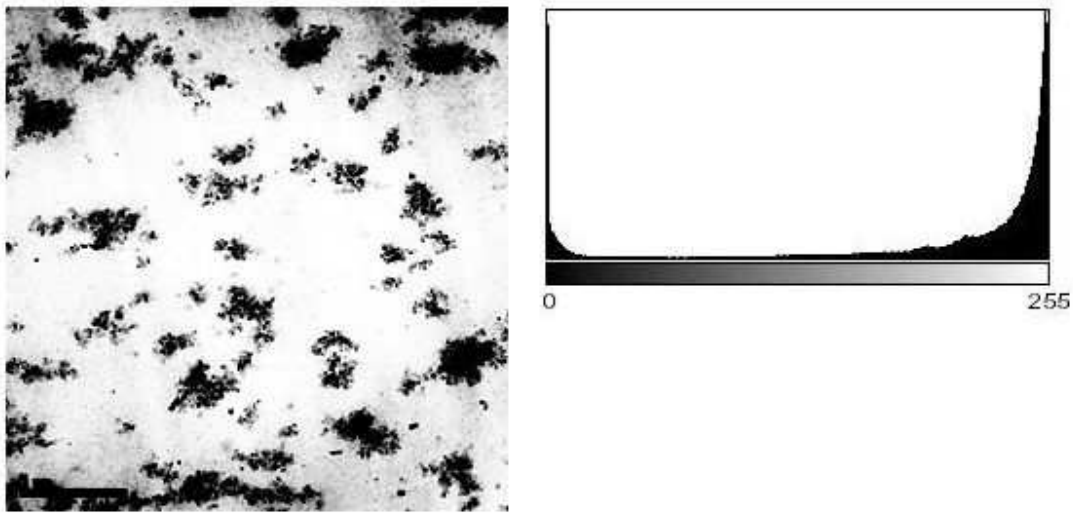

Figure 3: Image analysis step 2b (image enhancement): adjustment of brightness and contrast

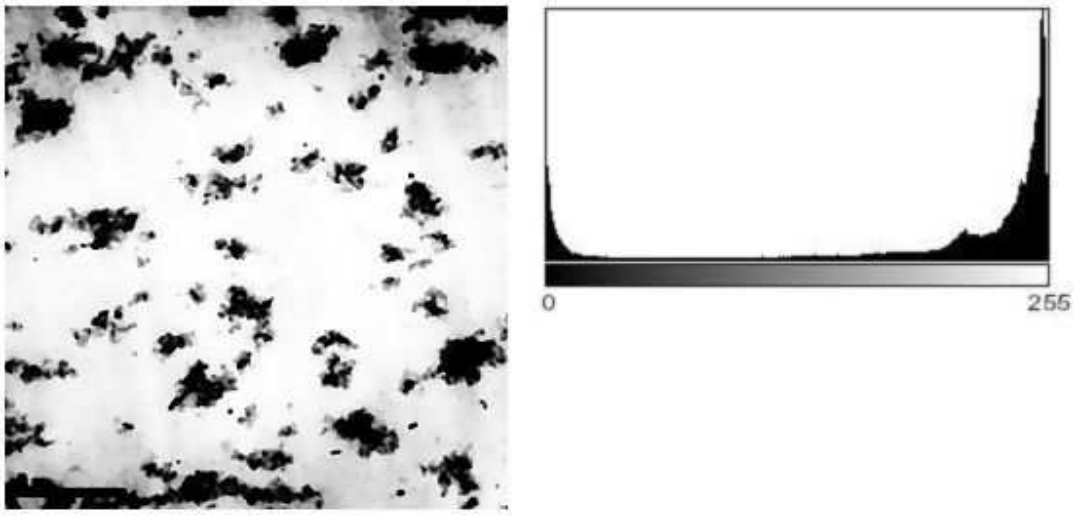

Figure 4: Image analysis step 2c (image enhancement): filling of agglomerates

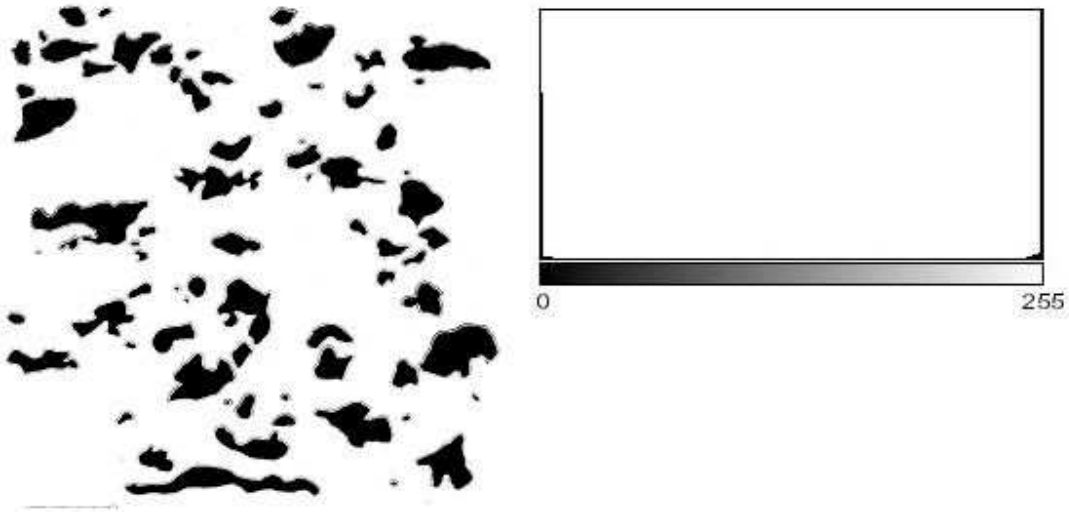

Figure 5: Image analysis step 3 (image thresholding): creation of a binary image

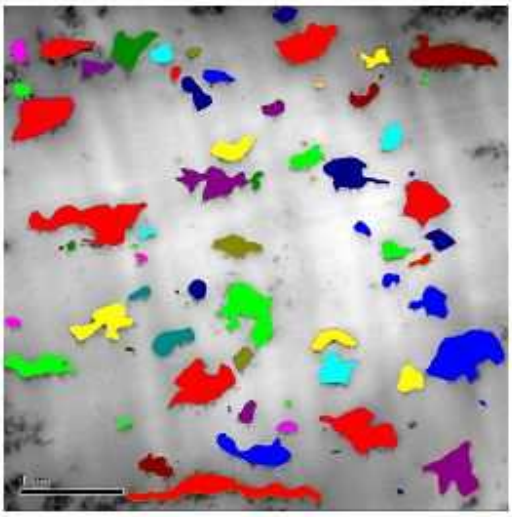

Figure 6: Image analysis step 4 (identification of the aggregates): colors are used to highlight separated aggregates

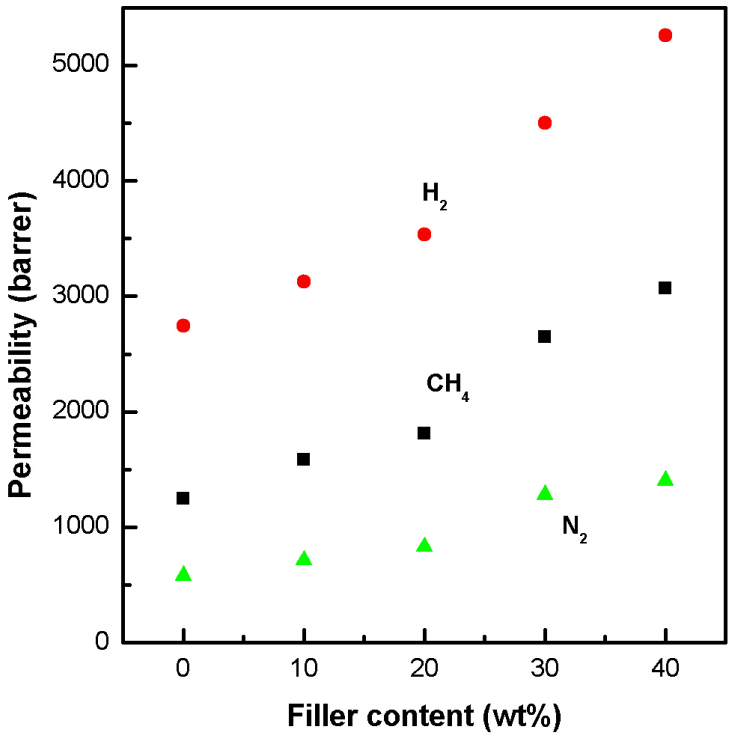

Figure 7: Nitrogen (triangle), hydrogen (circle) and methane (square) permeability as a function of filler content

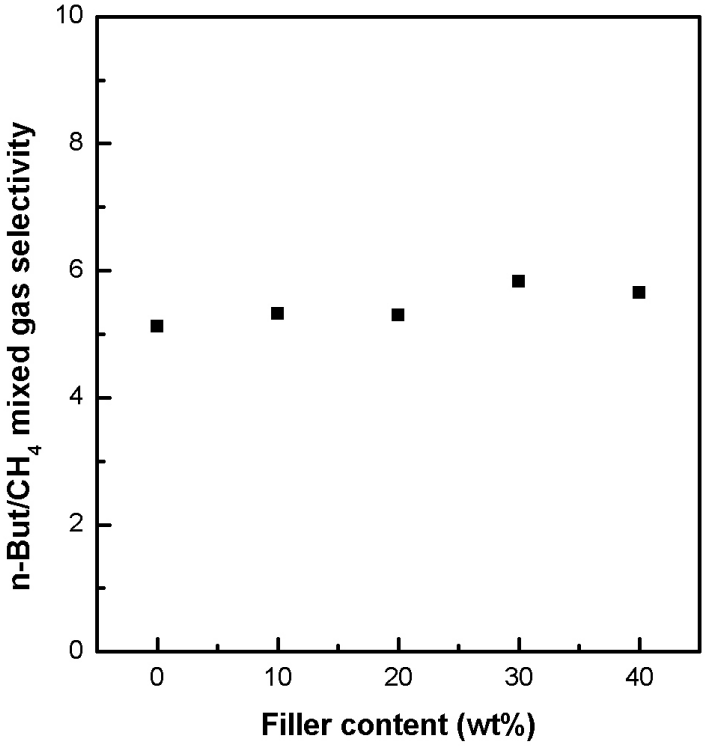

Figure 8: n-Butane/methane mixed gas selectivity, with a feed mixture of 2 vol% butane in methane, as a function of filler content

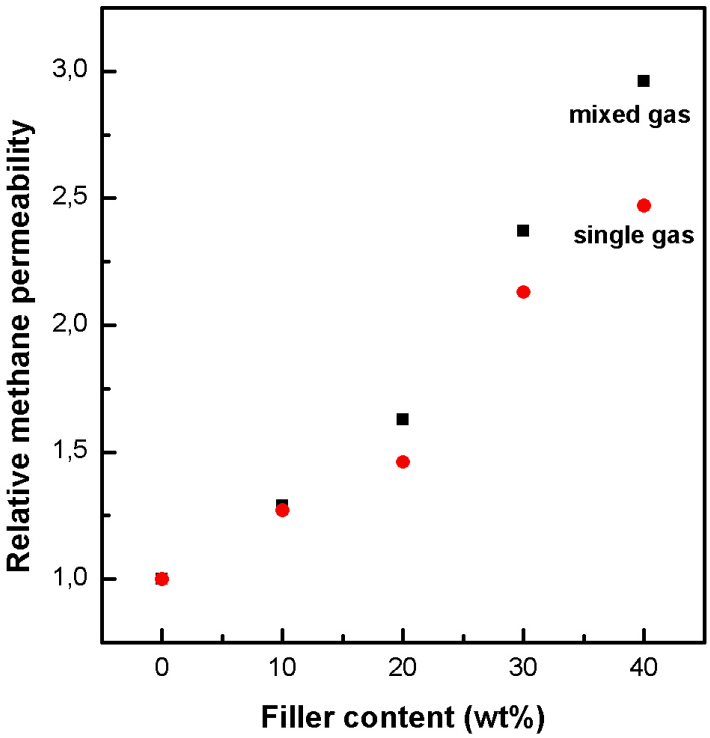

Figure 9: Relative mixed (square) and single (circle) gas methane permeability as a function of filler content

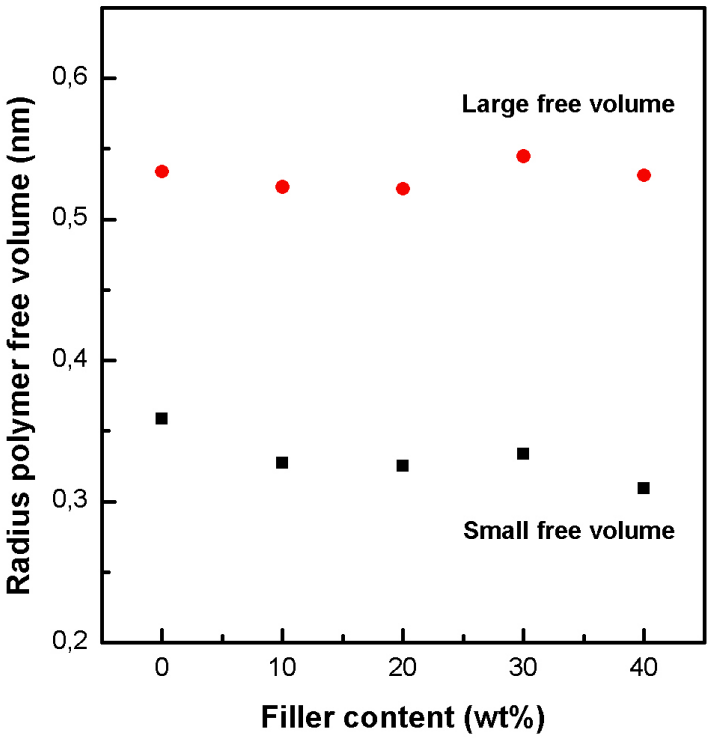

Figure 10: Small (square) and large (circle) free volume cavity radius in PMP/silica nanocomposites as a function of filler content

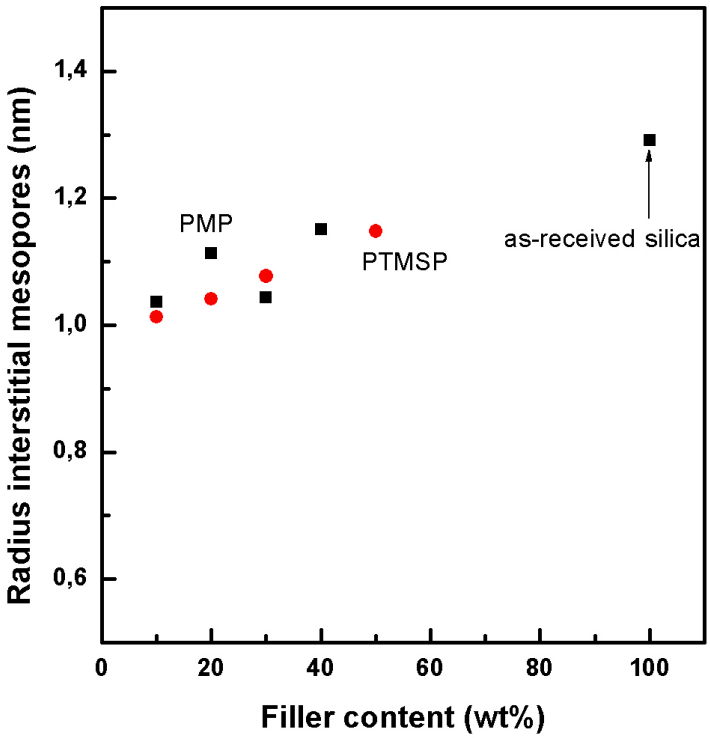

Figure 11: Interstitial cavity radius in PTMSP/silica (circle) and PMP/silica (square) nanocomposites as a function of filler content

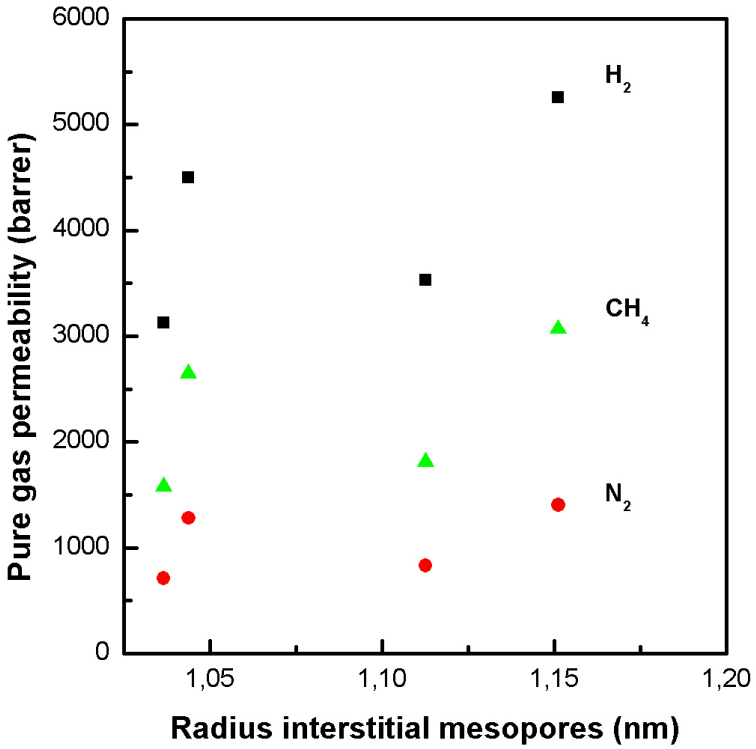

Figure 12: Nitrogen (circle), hydrogen (square) and methane (triangle) permeability as a function of interstitial cavity size

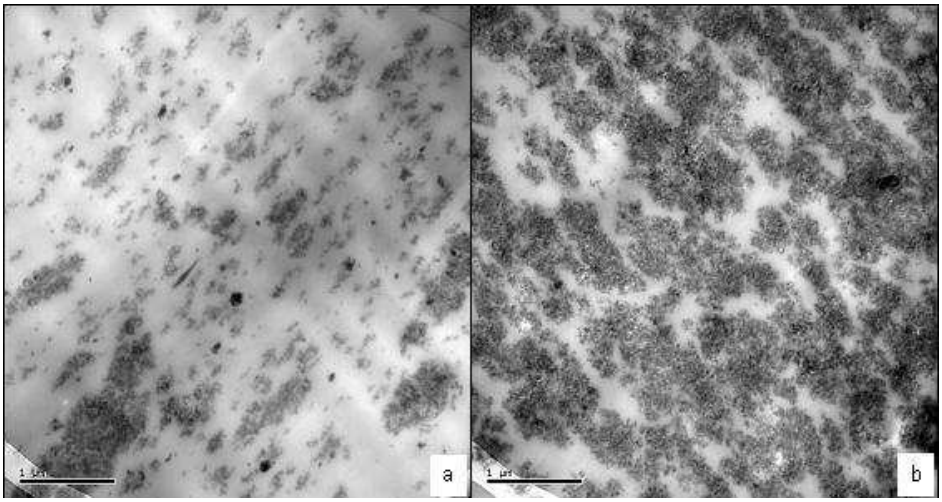

Figure 13: TEM pictures of PMP membranes filled with (a) 10 and (b) 30 wt% silica

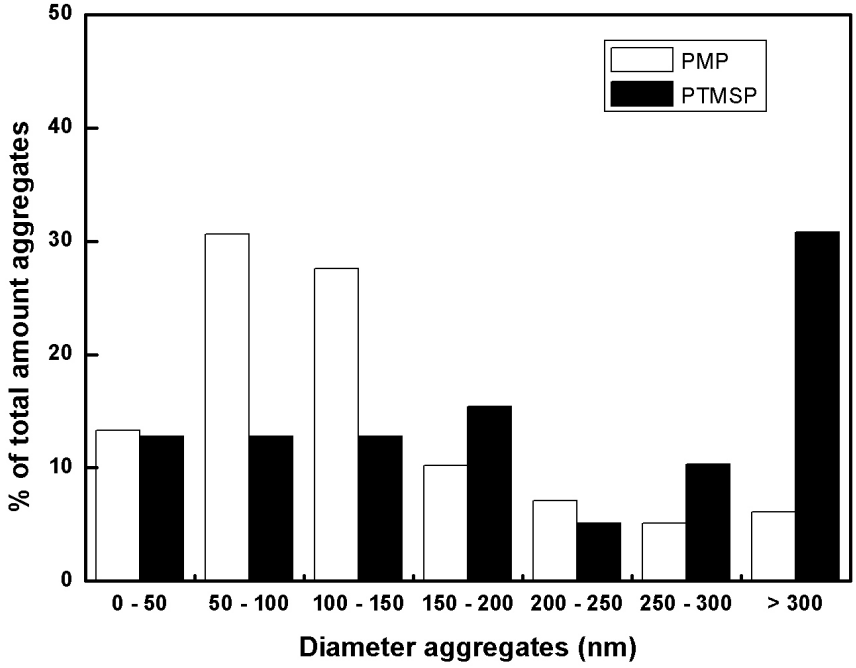

Figure 14: Percentage of the total amount of silica aggregates as a function of the diameter of the aggregates

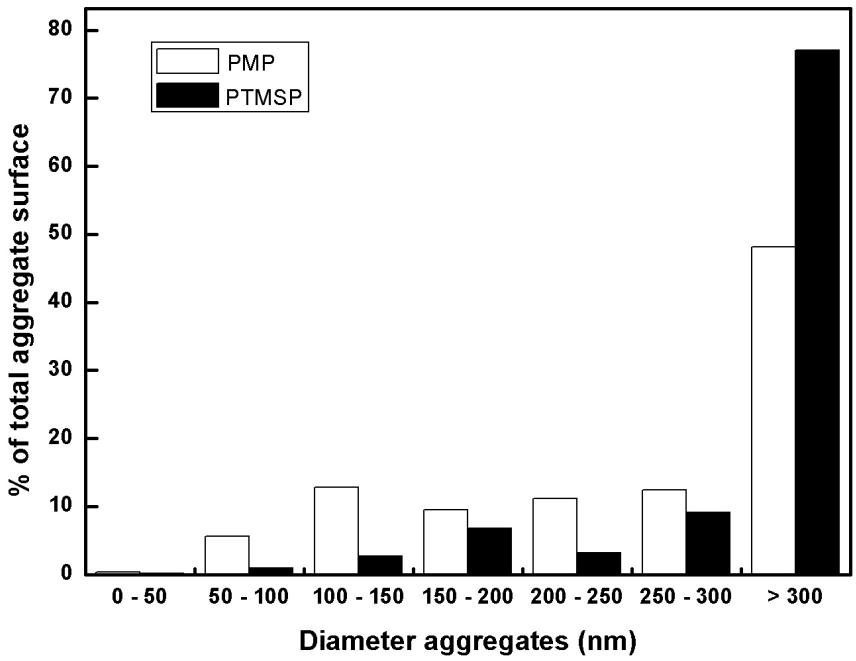

Figure 15: Percentage of the total aggregate surface taken by aggregates with a certain diameter

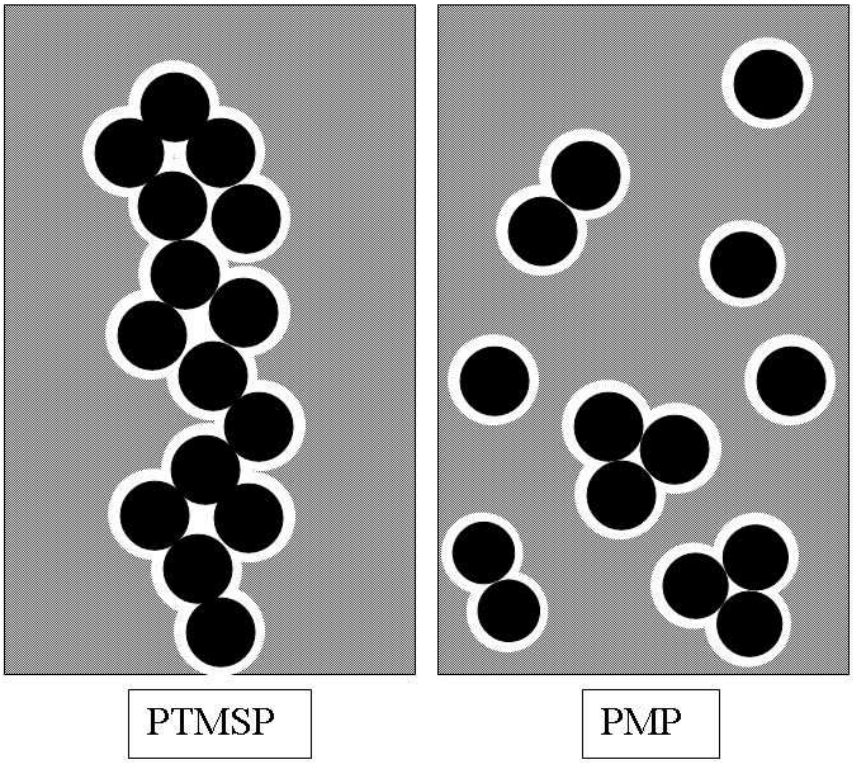

Figure 16: Schematical view of membrane structure of PTMSP/silica and PMP/silica nanocomposites